

AD-A195 989

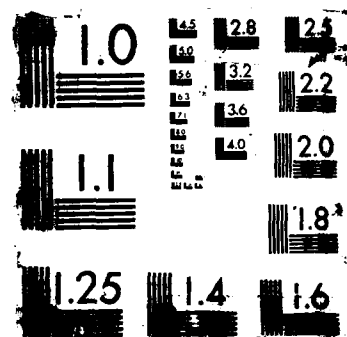
HYDROGEN EMBRITTLEMENT OF IRON-NICKEL ALLOYS(U)
ILLINOIS UNIV AT URBANA DEPT OF MATERIALS SCIENCE AND
ENGINEERING W Y CHU ET AL. APR 88 N00014-83-K-0460

1/1

UNCLASSIFIED

F/G 11/6.1 NL





DTIC FILE COPY

(4) (A)

AD-A195 909

DTIC
ELECTE
JUN 01 1988
S D

HYDROGEN EMBRITTLEMENT OF IRON-NICKEL ALLOYS

W.Y. CHU AND H.K. BIRNBAUM

University of Illinois
Materials Research Laboratory
and
Department of Materials Science and Engineering
Urbana, IL 61801

TECHNICAL REPORT
April 1988

Office of Naval Research
Contract USN 00014-83-K-0468

DISTRIBUTION STATEMENT A
Approved for public release;
Distribution Unlimited

This document is unclassified. Reproduction and distribution for any purpose of the U.S. Government is permitted.

88 6 1 063

HYDROGEN EMBRITTLEMENT OF IRON-NICKEL ALLOYS

W.Y. Chu and H. K. Birnbaum
University of Illinois
Department of Materials Science
and
Materials Research Laboratory
Urbana, IL 61801

ABSTRACT

The effects of hydrogen on the deformation and fracture of alloys in the Fe-Ni alloy system were studied as a function of the alloy composition and the amount of sulfur segregated at the grain boundaries. A ductile to brittle transition in the tensile parameters and in the fracture mode was observed as the hydrogen fugacity was increased during the deformation. The variation of this transition fugacity with segregated sulfur and with the alloy concentration was studied. The results were related to the mechanisms proposed for hydrogen related fracture of metals.



Accession For	
NTIS CRA&I	<input checked="checked" type="checkbox"/>
DTIC TAB	<input type="checkbox"/>
Unannounced	<input type="checkbox"/>
Justification	
By <u>per HP</u>	
Distribution /	
Availability Codes	
Dist	Avail and/or Special
A-1	

INTRODUCTION

In many alloy systems, hydrogen embrittlement under relatively high fugacity conditions occurs by intergranular fracture. One of these is the Fe-Ni alloy system which exhibits intergranular hydrogen related fracture when tested with a high supersaturation of solute hydrogen or while being cathodically charged with hydrogen^{1,2}. The results obtained on this alloy system indicate that the hydrogen embrittlement susceptibility decreases as the iron concentration of the alloy increased^{1,2}. While there is no known basis for this phenomenon, it is of significance as the Fe-Ni system is the basis of many commercially important alloy systems. These early measurements contained no information about the grain boundary chemistry and it is known that the effects of hydrogen are generally sensitive to the concentrations of other elements at grain boundaries.

One particular element, ^{Sulphur}S, is known to increase the susceptibility of ^{Nickel}Ni and its alloys^{3,4,5,6,7} and Fe and its alloys^{8,9,10} to hydrogen embrittlement although the mechanism of this increased susceptibility is not known. Yoshino and McMahon⁸ suggested that the cohesive energy of the prior austenitic grain boundaries in steel were decreased by the presence of both S and H and that the plasticity which accompanies fracture is also decreased¹¹. While a direct demonstration of the decrease of the cohesive energy by either segregated S or H has not been obtained, the decrease of plasticity which accompanies S segregation at grain boundaries in Ni has been directly observed⁷. Similar conclusions were drawn by Shin and Meshii on pure iron¹⁰ who suggested that the effects of each element on the fracture were independent and additive. Both of these experiments utilized solute hydrogen for the embrittlement. In the case of hydrogen introduced from an aqueous solution, it was suggested³ that the presence of metalloids such as S at the grain boundaries caused intergranular embrittlement by facilitating the entry of hydrogen with the metalloids acting as hydrogen recombination poisons at the metal surface; implying that the effects are synergistic rather than simply additive.

It is difficult to determine whether the effects of the segregated S and hydrogen are additive or synergistic on the basis of the available results. The measurements of Breummer et al^{4,5,9} clearly show that the hydrogen fugacity during cathodic charging which is necessary for intergranular fracture of Ni and Fe decreases as the amount of S segregated at the grain boundaries increases. Similar effects have been shown for solute hydrogen in Ni where the amount of hydrogen required for intergranular fracture is greatly decreased by even partial monolayer S segregation^{5,6}. These effects could result from a decrease in the "cohesive energy" by H and S or from changes in the amount of hydrogen segregated at the grain boundaries by the presence of segregated S. The latter has been clearly demonstrated at external surfaces of Ni by Fukushima and Birnbaum using Secondary Ion Mass Spectrometry. Hydrogen segregation at external surfaces was shown to extend over significant distances from the surface and segregated S increased the amount of H segregated in the vicinity of the surface. Segregation of H at grain boundaries has been demonstrated¹² but is much more difficult to quantify.

Another factor which makes the interactions of hydrogen and sulfur difficult to understand is that the mechanism of intergranular fracture is not established. In a number of systems it was shown that hydrogen related fracture occurred by hydrogen enhanced localized plastic processes in the vicinity of the grain boundaries rather than directly at the grain boundaries. On the basis of hydrogen enhanced dislocation motion, sulfur segregated at the grain boundaries can have several effects on hydrogen related intergranular fracture. Segregated S increases the concentration of hydrogen segregated in the vicinity of the grain boundary thus causing enhancement of the localized plasticity and the localized plastic fractures. In addition, the segregated S may of itself decrease the bonding across the grain boundary. The effects of both S and H on intergranular fracture would be expected to be non-linear, ie. the effect of both solutes present at the same time would be greater than the additive individual effects of the solutes considered separately.

An alternative view of the effects of hydrogen on fracture is that it causes a decrease in the atomic bond strength, ie. decohesion^{15,16}. Sulfur is also predicted to have the effect of weakening the atomic bonding across grain boundaries^{15,16}. On this basis the effects of both S and H present in the materials would be expected to be additive where there is no effect on hydrogen segregation due to S segregation and greater than additive if S enhances H segregation at the grain boundaries.

The present experiments examine some of these questions with particular relevance to the Fe-Ni system. In addition, the effect of alloy composition on the susceptibility to hydrogen embrittlement in this system is determined taking the sulfur segregation into account.

EXPERIMENTAL PROCEDURES

The alloys used in the present study were prepared by vacuum melting, casting into ingots, and hot rolling to plates 6.4 mm thick. These were then cold rolled into strips 0.25 mm thick from which "dog-bone" shaped tensile specimens were machined. The tensile axis was parallel to the rolling direction. The compositions of the alloys used in this study were determined by analysis with the C,S,N, and O values being measured by vacuum extraction and are given in Table I.

Table I ALLOY COMPOSITION (at. %)

Alloy	C	S	N	O	Grain Size (micrometers)
Ni	0.005	0.0011	0.0021	0.012	46
75Ni25Fe	0.025	0.0024	0.0033	0.0094	62
75Ni25Fe-low S	—	0.0007	0.0033	0.0094	62
50Ni50Fe	0.045	< 0.001	< 0.002	0.0064	40
30Ni70Fe	0.007	0.0048	0.0057	—	55

All specimens were solution treated for 0.5 hrs. in vacuum at 1273 K followed by an oil quench without removing the specimen from the vacuum. This anneal established the grain sizes which are also listed in Table I. As described in the text, some specimens were annealed at 973 K for 30 min. following the anneal at 1273 K to increase the amount of S segregated at the grain boundaries. In addition, some specimens were annealed at various temperatures below 1273 K immediately after cold rolling and these had grain sizes which increased to the values given in Table I as the annealing temperatures were increased.

Hydrogen was introduced before deformation by either free corrosion in solutions of H_2SO_4 (0.2 N, pH=1; 1 N, pH=0.3; or 1N H_2SO_4 plus 10 mg/L NaAsO₂) as specified in the text or by cathodic charging at various current densities in 1N H_2SO_4 plus 10 mg/L NaAsO₂. All the precharging was carried out for 24 hrs.; a time greater than that required for hydrogen diffusion across the specimen thickness.

After precharging the specimens were tensile tested at room temperature at a strain rate of $6.2 \times 10^{-6} \text{ s}^{-1}$ while the same hydrogen charging condition as used in the precharging was maintained. (Uncharged specimens were strained at a strain rate of $2.2 \times 10^{-3} \text{ s}^{-1}$ as tests showed that the ductility and fracture behavior was insensitive to strain rate in this range.) In many cases several specimens were tested under identical conditions and the results reported are averages of the individual behaviors.

After fracture the specimens were examined in an SEM and the mode of fracture was determined. The percent of intergranular fracture was determined by a linear intercept method. The grain boundary chemistry was studied by Auger Electron Spectroscopy (AES) on hydrogen charged specimens which were fractured in the AES vacuum. Measurements were made on intergranular fracture facets with the compositions being determined using standard sensitivity factors. the values quoted are the average of at least six measurements on different grain facets.

All of the alloys studied were single phase fcc gamma in structure as expected from the published phase diagram¹⁷ and from the fact that they were heat treated and quenched from above 773 K. The M_s temperatures were all below about 223 K¹⁸ and therefore no martensite was expected to form on quenching. Metallographic examination of the alloys confirmed that no martensite formed and that the alloys were all single phase.

EXPERIMENTAL RESULTS AND DISCUSSION

The tensile parameters for the 75Ni25Fe alloy which was quenched from 1273 K depended on the cathodic charging current density as shown in Fig. 1. All of the parameters characteristic of uncharged specimens were characteristic of specimens which were tested at a free corrosion potential obtained by immersion of the specimens in 1N H_2SO_4 containing 10 mg/L NaAsO₂. As the cathodic precharging and charging potential was increased the strain to failure and the Ultimate Tensile Strength showed a very sharp ductile - brittle transition at about 2 A/m². The fracture mode, measured by the percent intergranular fracture (Figs. 1 and 2) showed a similar transition with a completely intergranular fracture being observed at cathodic currents $i > 2$ A/m². The effects of hydrogen charging were reversible on vacuum outgassing at 423 K for 24 hours for specimens which had been precharged at $i < 20$ A/m² (Fig. 1). The fracture mode reverted to a microvoid coalescence ductile fracture on outgassing as shown in Fig. 2d. At higher cathodic current densities a permanent damage appears to have occurred as seen by the decrease in strain to failure and the intergranular fracture which remains after outgassing.

Hydrogen effects in this 75Ni25Fe alloy appear to be associated with the segregation of S at the grain boundaries. Analysis of the grain boundary facets of this alloy after quenching from 1273 K, cathodic charging, and fracture in the AES showed an average grain boundary concentration of S of 2.3 at. %. A small amount of C was also detected on the fracture surfaces.

Specimens of this alloy were annealed in H_2 at 1173 K for 200 hours to reduce the S concentration from 24 at. ppm to 7 at. ppm (these specimens were denoted 75Ni25Fe-low S) and were then quenched from 1273 K and tested during cathodic charging after precharging at various cathodic current densities in exactly the same manner as for the unpurified specimens. Results of these tests are shown in Fig. 3 where it is seen that the ductile - brittle transition is much more gradual in the low S purified specimens; the cathodic current density corresponding to a loss of ductility of 50% was 4 A/m². The AES analysis of the intergranular fracture surfaces indicated a S concentration of < 0.1 at. % and that the C concentration at the surface was about the same as in the unpurified specimens.

Since sulfur segregation can cause intergranular embrittlement in the absence of hydrogen if it is extensive enough, this factor was examined for the 75Ni25Fe alloy

containing 24 at. ppm S. The results are shown in Fig. 4 for specimens tested in air without hydrogen charging. These specimens were cold rolled from a thickness of 0.75 mm to 0.25 mm prior to the anneals and hence recovered and recrystallized during the anneals. The specimens were completely brittle and exhibited completely intergranular fracture after 30 min. anneals at temperatures between 723 and 973 K. As the temperature of the anneals were increased, the grain size of the specimens also increased. Analysis of the fracture surfaces by AES after the 973 K anneal showed a S concentration of 18.3 at. % indicating that at these low annealing temperatures a grain boundary sulfide probably formed. The strain to failure increased and the amount of intergranular fracture decreased as the annealing temperature was increased further; reaching the completely ductile values at annealing temperatures above 1173 K.

Specimens which had been annealed at 1273 K after cold rolling could be embrittled by annealing for 30 min. at lower temperatures (Fig. 4) with a ductility minimum being observed at annealing temperatures of about 1023 K. For these specimens, the grain size was established to be an average of 60 micrometers by the 1273 K anneal. At the ductility minimum the fracture was completely intergranular and the strain to failure was reduced from about 48% to about 20%. The grain boundary S concentration was 7.1 at. % after a 973 K anneal again indicating the presence of a grain boundary sulfide. For a constant annealing time of 30 min. the ductility recovers and the amount of intergranular fracture decreases as the annealing temperature was further decreased.

In considering these results it is important to realize that based on the kinetics of S segregation to surfaces in Ni and Fe none of the above anneals were sufficient to achieve equilibrium S segregation at the grain boundaries during the 30 minute anneals. The ductility minimum observed in the pre-annealed specimens is a consequence of the increased tendency for intergranular segregation of S as the temperature of the segregation anneal is decreased and the decrease in the S diffusivity as the temperature is decreased. The ductility below the observed minimum would continue to decrease if the anneals were prolonged and the concentration of S at the grain boundaries allowed to increase towards its equilibrium value. This appears to be observed for the specimens which were undergoing recovery and recrystallization during the segregation anneals; perhaps as a result of the increased S diffusivity caused by the dislocations and point defects in the cold worked structure.

As previously indicated, the effect of hydrogen on the fracture of these alloys depends on the level of the grain boundary hydrogen concentration (Figs. 1 and 3). This is shown more clearly in Fig. 5 for various heat treatments of the 75Ni25Fe and 75Ni25Fe-low S alloys. In the as annealed condition, specimens containing <0.1 and 2.3 at. % S at the grain boundaries and which were tested in air without any hydrogen being introduced (point A in Fig. 5) exhibited 100 % microvoid coalescence ductile failure; although the strain to failure was reduced in the higher S specimens. Increasing the amount of S segregated at the grain boundaries to 7.1 at. % resulted in

a further decrease of the strain to failure and a mixed intergranular - ductile fracture while alloys containing 18.3 at. % S at the grain boundaries were completely brittle and fractured in a completely intergranular mode. Under freely corroding conditions in a H_2SO_4 solution of $\text{pH} = 1$ (point B in Fig. 5) aging for 24 hours and testing in the solution had no effect on the behavior of any of these specimens. In a $\text{pH} = 0.3$ H_2SO_4 solution, testing under free corrosion conditions after a 24 hr. exposure (point C in Fig. 5) resulted in a decrease in the strain to failure and an increase of the intergranular fracture for specimens having 7.1 at. % S at the grain boundaries. A somewhat more severe charging condition, free corrosion for 24 hrs. and testing in 1 N H_2SO_4 containing 10 mg/L NaAsO_2 , resulted in a further decrease in the ductility of the 7.1 at. % grain boundary S specimen but had no effect on the specimens having less grain boundary segregated S. As the hydrogen charging conditions were increased in severity all of the specimens showed a ductile - brittle transition with the transition being increasingly sharp and occurring at lower cathodic charging currents as the grain boundary sulfur concentration was increased.

Results, very similar to the above, were observed for an alloy having the composition 30Ni70Fe which contained 48 at. ppm S in solution. After quenching from 1273 K the grain boundary concentration of S was < 0.1 at. % (in contrast to the 75Ni25Fe specimen containing 24 at. ppm S and which had 2.3 at. % S segregated to the grain boundaries after the quench from 1273 K). The grain boundary S concentration increased to 4.9 at. % on aging at 973 K (compared to 7.1 at. % S in the 75Ni25Fe alloy). It appears from these results that the 30Ni70Fe alloy exhibited less tendency for S segregation to the grain boundaries than the 75Ni25Fe alloy.

After quenching from 1273 K, the 30Ni70Fe alloy exhibited completely ductile behavior with a ductile microvoid coalescence fracture under the conditions of precharging and charging at current densities $< 10 \text{ A/m}^2$ during deformation. During straining while charging at current densities above 10 A/m^2 , a sharp transition to brittle behavior and intergranular fracture occurs (Fig. 6). The hydrogen effects appear to be reversible below current densities of about 20 A/m^2 . Aging at 973 K for 30 minutes to increase the concentration of S at the grain boundaries resulted in an increased susceptibility to hydrogen embrittlement (Fig. 6) as previously observed for the 75Ni25Fe composition. For these specimens a significant loss of ductility and increase in intergranular fracture was noted on free corrosion for 24 hrs. and tensile testing in H_2SO_4 solutions having pH of 2 or less and on cathodic charging as the current density was increased.

These effects of hydrogen charging were reversible as seen in Fig. 6. Vacuum outgassing after precharging at current densities below about 20 A/m^2 caused a complete recover of the ductility and the fracture mode become ductile microvoid coalescence rather than intergranular. Even at current densities above 20 A/m^2 the recovery of the ductility and fracture mode on vacuum outgassing was almost complete.

Table II VARIATION OF HYDROGEN FUGACITY REQUIRED FOR
DUCTILE - BRITTLE TRANSITION WITH S SEGREGATION

Alloy	Grain boundary S Concentration (at. %)	Condition for 50% Loss In Ductility	Onset of Loss of Ductility
Ni	—	Cathodic charging; $\sim 8 \text{ A/m}^2$	$\sim 0 \text{ A/m}^2$
75Ni25Fe	2.3	Cathodic charging; 2 A/m^2	$\sim 2 \text{ A/m}^2$
75Ni25Fe	7.1	Free corrosion; $\text{H}_2\text{SO}_4, \text{pH}=0.3$	$\text{H}_2\text{SO}_4, \text{pH}=1$
75Ni25Fe	18.3	No H charging required	----
75Ni25Fe - low S	<0.1	Cathodic charging; 4 A/m^2	$\sim 0 \text{ A/m}^2$
50Ni50Fe	—	Cathodic charging; $\sim 50 \text{ A/m}^2$	$\sim 0 \text{ A/m}^2$
30Ni70Fe	<0.1	Cathodic charging; 10 A/m^2	$\sim 10 \text{ A/m}^2$
30Ni70Fe	4.9	Free corrosion; $\text{H}_2\text{SO}_4, \text{pH}=0.3$	$\text{H}_2\text{SO}_4, \text{pH}=2$

Despite the very large difference in the alloy compositions, the 75Ni25Fe and 30Ni70Fe alloys discussed above show very similar behaviors on exposure to high hydrogen fugacity environments. Under heattreatment conditions which lead to low S segregation at the grain boundaries the ductile - brittle transition occurs at relatively "high" hydrogen fugacities as measured by the cathodic charging currents while conditions which increase the S segregation at the grain boundaries decrease the hydrogen fugacity required for intergranular fracture as shown in Table II. This pattern of behavior is the same as that previously reported for pure Ni^{5,6} and Fe^{3,5,9,10}. It is difficult to make detailed comparisons between the two alloy compositions as the level of grain boundary sulfur segregation in the 30Ni70Fe and in the 75Ni25Fe-low S alloys are below the level measurable by the AES method. However, the data indicate that the level of S segregation is more important than the alloy composition. Differences observed in the hydrogen susceptibility of various alloy compositions may reflect the S segregation enthalpy and/or kinetics rather than the interactions with hydrogen. Both of these may depend on alloy composition and result in different S concentrations at the grain boundaries during similar heat treatments; as discussed above.

The results for each of the alloys (Table II) is similar to that obtained by Breummer et al^{4,5,9} for cathodic charging of Fe and Ni and by Lassila and Birnbaum⁶ for hydrogen in solid solution in Ni. The increased segregation of S at grain boundaries

decreases the amount of hydrogen required for intergranular embrittlement. The detailed relationships between S and H concentrations at the grain boundaries have not been determined. It is however well established that grain boundary S concentrations of the order of monolayers or less do not of themselves cause intergranular fracture in the absence of segregated hydrogen ⁶. This conclusion is consistent with the results shown in Fig. 5 where it is seen that in the absence of hydrogen charging (points A) a grain boundary sulfur concentration of 2.3 at. % (curve 2) leads to a significant decrease in strain to failure without significant amounts of intergranular fracture. Larger amounts of segregated S (curves 3 and 4) further decrease the strain to failure and exhibit large increases in the amount of intergranular fracture; possibly as a result of the formation of grain boundary sulfides. At higher H fugacities, effects of hydrogen on the loss of ductility and the amounts of grain boundary fracture are noted even in specimens with small segregated S levels.

At low hydrogen fugacities the effects of both segregated S and H are greater than additive as seen from the data shown in Fig. 5. The effects of segregated S alone are given by the data at points A while the effect of hydrogen alone is given by curve 1. At cathodic charging currents of the order of 2 A/m², for example, the effect of segregated S and hydrogen, curve 2, leads to a ductility loss of about 85% and about 100% intergranular fracture. These values may be compared to a 15% loss of ductility due to segregated S with 0% intergranular fracture and about 25% loss of ductility and 40% intergranular fracture due to H. The sum of these effects is less than observed for the tests with both segregated S and H. This nonlinear effect may result from the increased segregation of H due to the presence of S at the grain boundaries ^{12,6}. At higher concentrations of segregated S or higher H fugacities, the effects of S and H tend to be additive. This is a natural consequence of the saturation of the ductility loss and the amount of intergranular fracture at 100% each.

Despite the above uncertainties about the relative roles of S segregation and alloy composition on hydrogen susceptibility, there does seem to be a significant effect of the alloy composition in the Fe-Ni system. This is shown by the data in Fig. 7 for the 50Ni50Fe composition which has a very low S concentration. This alloy exhibits a decrease in ductility and an increase in the amount of intergranular fracture at very low cathodic current densities (characteristic of high grain boundary segregated S concentrations) but the transition is very gradual; at high current densities appreciable ductility remains and the fracture is only partially intergranular (characteristic of low grain boundary segregated S concentrations). It was not possible to determine the grain boundary S concentration in these alloys as they did not fracture intergranularly under the conditions in the AES.

The behavior of the 50Ni50Fe alloy was similar to that of "pure" Ni specimens which contained 11 at. ppm S. As shown in Fig. 8, Ni specimens quenched from 1273 K exhibited the onset of ductility loss at low cathodic current densities but the transition to a "brittle" behavior and to intergranular fracture was very gradual; a behavior similar to that seen in the 50Ni50Fe alloy but strikingly different that seen

in the other compositions. In the case of Ni specimens, there was evidence for ductility loss as a result of free corrosion in the 1N H₂SO₄ + 10 mg/L NaAsO₂ electrolytic charging solution. As in the 50Ni50Fe alloy, appreciable ductility and microvoid coalescence fracture remained for tests carried out at high current densities.

In the case of the pure Ni specimens the grain boundary sulfur concentration could also not be determined as it was not possible to fracture the specimens intergranularly in the AES system. However, for Ni containing 11 appm S the amount of segregated S after a 30 min. anneal at 1273 K is expected to be quite small¹⁹. The low amount of intergranular fracture shown in Fig. 8 is consistent with the previous studies^{5,6} which show that in the presence of low S concentrations at the grain boundaries a high H fugacity is required for intergranular fracture.

Hydride formation on the surface of the Ni specimens was noted for current densities above about 20 A/m², consistent with many other observations, while hydrides were not observed for any of the other alloy compositions.

CONCLUSIONS

1. Hydrogen introduced by cathodic charging appears to have a significant embrittling effect, measured by a loss of strain to fracture and by the extent of intergranular fracture, for all compositions in the fcc gamma phase region of the Ni-Fe alloy system. The susceptibility of the alloys to hydrogen embrittlement appears to be least for the 50% Ni - 50% Fe alloy and for pure Ni.
2. The extent of hydrogen embrittlement is related to the amount of grain boundary segregation of sulfur; increasing as the extent of S segregation increases. The sharpness of the ductile to brittle transition with hydrogen is greatest for the high S segregated alloys and the hydrogen fugacity at which the transition occurs decreases as S segregation increases.
3. At low S segregation and hydrogen fugacities the effects of both elements on fracture appear to be greater than additive.

ACKNOWLEDGEMENTS

This research was supported by the Office of Naval Research through contract USN 00014-83-K-0468. The authors would like to acknowledge the assistance of Dr. Barbara Ladna in carrying out the AES measurements. The facilities of the Center for Microanalysis of Materials were used for the AES experiments.

REFERENCES

1. P. Blanchard and A.R. Troiano: *Mem. Sci. Rev. Met.*, 1960, vol. 57, pp. 409-422.
2. M.L. Wayman and G.C. Smith: *Acta Metall.*, 1971, vol. 19, 227-231.
3. R.M. Latanision and H. Oppenheimer, Jr.: *Metall. Trans. A*, 1974, vol. 8A, pp. 483-492.
4. S.M. Bruemmer, R.H. Jones, M.T. Thomas and D.R. Baer: *Scripta Metall.*, 1980, vol. 14, pp. 1233-1237.
5. S.M. Bruemmer, R.H. Jones, M.T. Thomas, and D.R. Baer: *Metall. Trans. A*, 1983, vol. 14A, pp. 223-232.
6. D.H. Lassila and H.K. Birnbaum: *Acta Metall.*, 1987, vol. 35, pp. 1815-1822.
7. T.C. Lee, I.M. Robertson, and H.K. Birnbaum: *Acta Metall.* (In press).
8. K. Yoshino and C.J. McMahon, Jr.: *Metall. Trans. A*, 1974, vol. 5A, pp. 363-370.
9. S.M. Bruemmer, R.H. Jones, M.T. Thomas, and D.R. Baer: *Metall. Trans. A*, 1981, vol. 12A, pp. 1621-1629.
10. K.S. Shin and M. Meshii: *Acta Metall.*, 1983, vol. 31, pp. 1559-1566.
11. M.L. Jokl, V. Vitek and C.J. McMahon, Jr.: *Acta Metall.*, 1980, vol. 28, pp. 1479-1488.
12. H. Fukushima and H.K. Birnbaum: *Acta Metall.*, 1984, vol. 32, pp. 851-859.
13. I.M. Robertson, T. Tabata, W. Wei, F. Heubaum, and H.K. Birnbaum: *Scripta Metall.*, 1984, vol. 18, pp. 841-846.
14. T. Tabata and H.K. Birnbaum: *Scripta Metall.*, 1984, vol. 18, pp. 231-236.
15. R.P. Messmer and C.L. Briant: *Acta Metall.*, 1982, vol. 30, pp. 457-467.
16. M.E. Eberhart, K.H. Johnson, and R.M. Latanision: *Acta Metall.*, 1984, vol. 32, pp. 955-959.
17. M. Hansen: *Constitution of Binary Phase Diagrams*, McGraw-Hill Pub., New York, 1958, p. 677.
18. L. Kaufman and M. Cohen: *Trans. AIME*, 1956, vol. 206, pp. 1393-1401.
19. B. Ladna and H.K. Birnbaum: To be published.

FIGURE CAPTIONS

- Fig. 1 The effect of cathodic charging on the tensile properties and fracture mode of 75Ni25Fe alloy specimens. The data points at a current density of zero correspond to free corrosion and at A correspond to the uncharged condition. The data points on the curve labelled "outgassed" were obtained from specimens which were electrolytically charged with hydrogen for the same time and under the same conditions as the straining electrode test but were then given a vacuum outgassing treatment at 423 K for 24 hours.
- Fig. 2 SEM fractographs of the fracture surfaces of 75Ni25Fe specimens tested under various conditions. a) free corrosion in 1N H_2SO_4 + 10 mg/l NaAsO_2 , b) straining electrode test at a current density of 2 A/m^2 , c) straining electrode test at a current density of 8 A/m^2 , d) electrolytically charged at a current density of 8 A/m^2 followed by vacuum outgassing.
- Fig. 3 The effect of cathodic charging on the tensile properties and fracture modes of 75Ni25Fe-low S specimens. The data points at a current density of 0 correspond to free corrosion and at A correspond to the uncharged condition.
- Fig. 4 Strain to failure and fracture mode of 75Ni25Fe specimens tensile tested without hydrogen charging. - - - - Data is for specimens which were cold rolled before each of the indicated anneals. ——— Data is for specimens which were annealed at 1273 K before each of the anneals at the indicated temperatures.
- Fig. 5 Tensile deformation properties and fracture modes for 75Ni25Fe specimens heat treated to have various grain boundary S concentrations and then tested in straining electrode tests at various current densities. —●— 75Ni25Fe-low S specimens quenched from 1273 K; <0.1 at% S at the grain boundaries, - - -O- - - 75Ni25Fe specimens quenched from 1273 K; 2.3 at% S at the grain boundaries, —·—Δ—·— 75Ni25Fe specimens quenched from 1273 K followed by a 30 minute anneal at 973 K; 7.1 at% S at the grain boundaries, —·—□—·— 75Ni25Fe specimens annealed at 973 K immediately after cold rolling, 18.3 at% S at the grain boundaries. Test condition A is uncharged, B is under free corrosion in 0.2N H_2SO_4 (pH=1), C is under free corrosion in 1.0N H_2SO_4 (pH=0.3), 0 is under free corrosion in 1N H_2SO_4 with 10 mg/L of NaAsO_2 .
- Fig. 6 Tensile deformation properties and fracture modes for 30Ni70Fe specimens. ——— Specimens quenched from 1273 K; - - - - Specimens quenched from 1273 K and annealed at 973 K for 30 minutes, — - - — Specimens which were vacuum outgassed for 30 minutes at 423 K after precharging. Test condition A is uncharged, B is under free corrosion in 0.2N H_2SO_4 (pH=1), C is under free corrosion in 1.0N H_2SO_4 (pH=0.3), D is under free corrosion in H_2SO_4 (pH=2.0), 0 is under free corrosion in 1N H_2SO_4 with 10 mg/L of NaAsO_2 .

Fig. 7 Tensile properties and fracture modes for 50Ni50Fe specimens quenched from 1273 K. Test condition A is uncharged, 0 is free corrosion in 1N H₂SO₄ with 10 mg/L of NaAsO₂.

Fig. 8 Tensile properties and fracture modes for a pure Ni specimens quenched from 1273 K. Test condition A is uncharged, 0 is free corrosion in 1N H₂SO₄ with 10 mg/L NaAsO₂.

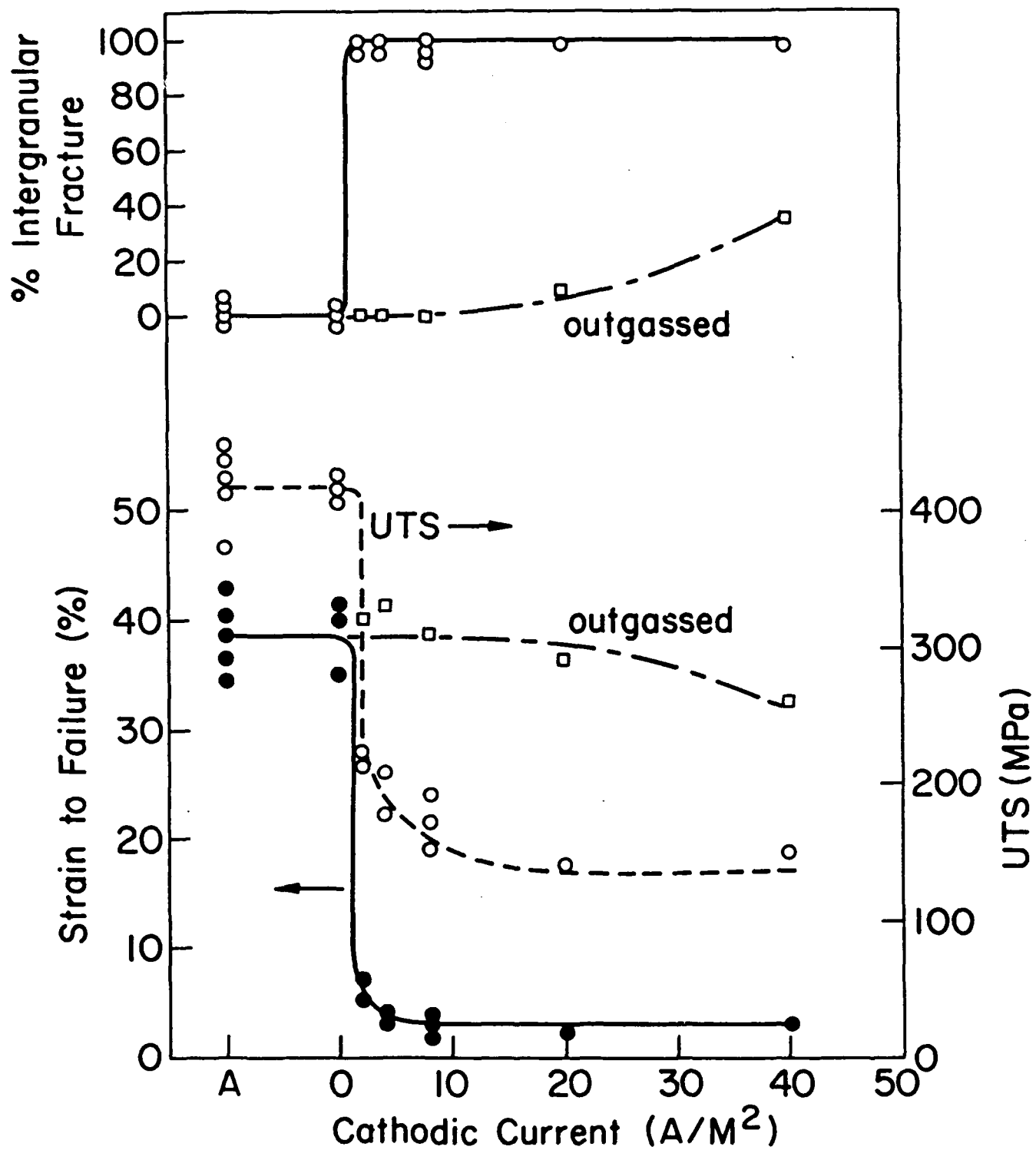


Fig. 1
Chu & Birnbaum

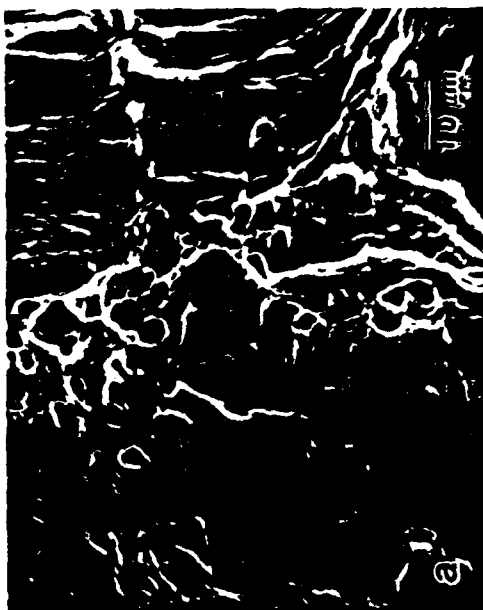
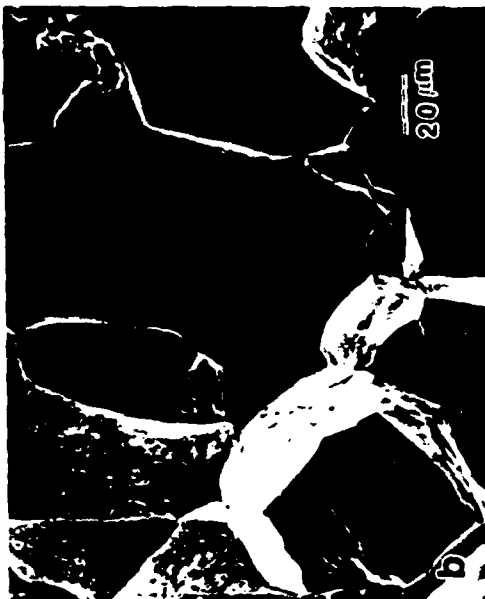


Fig. 2
Chu & Birnbaum

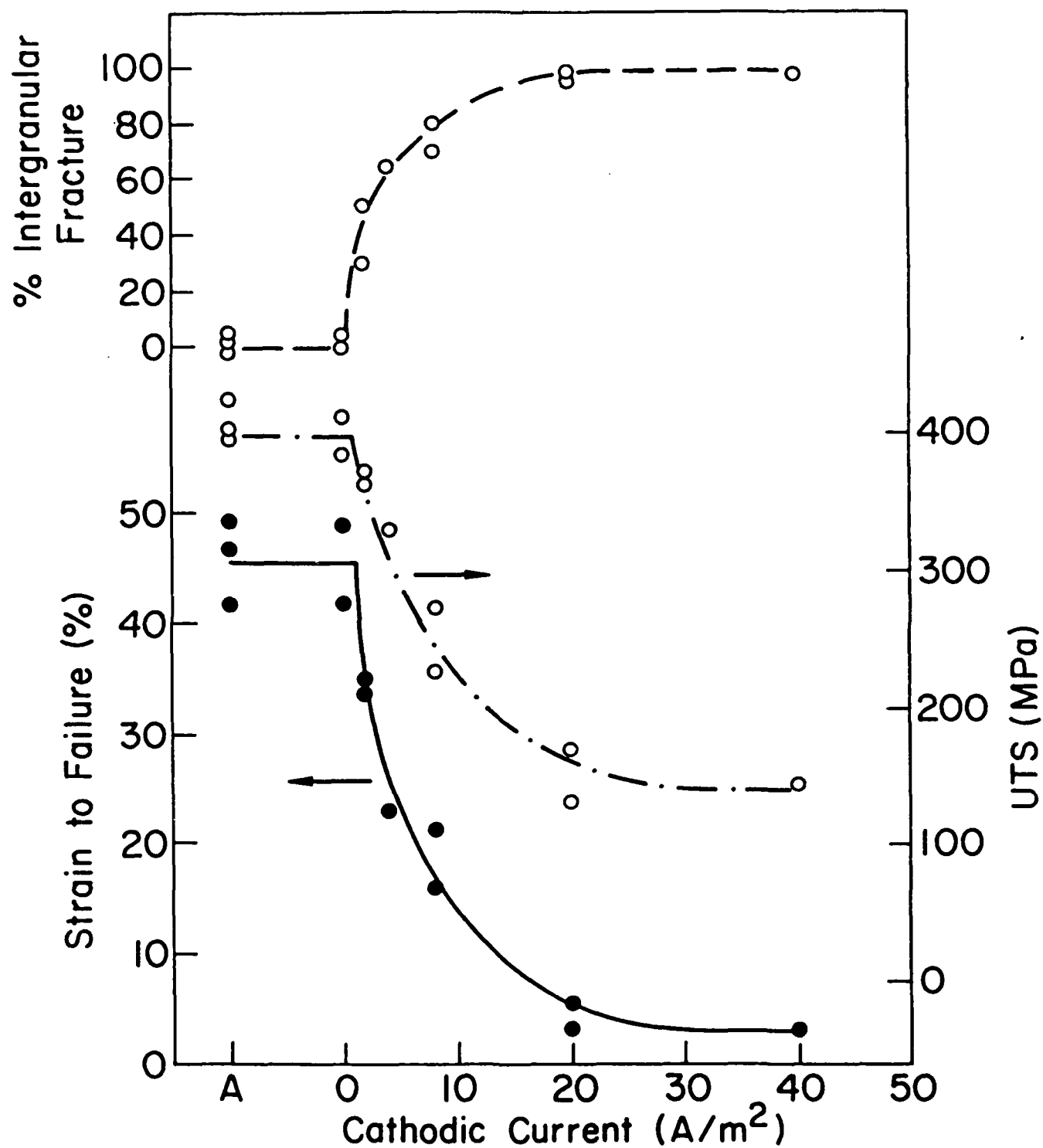


Fig. 3
Chu + Birnbaum

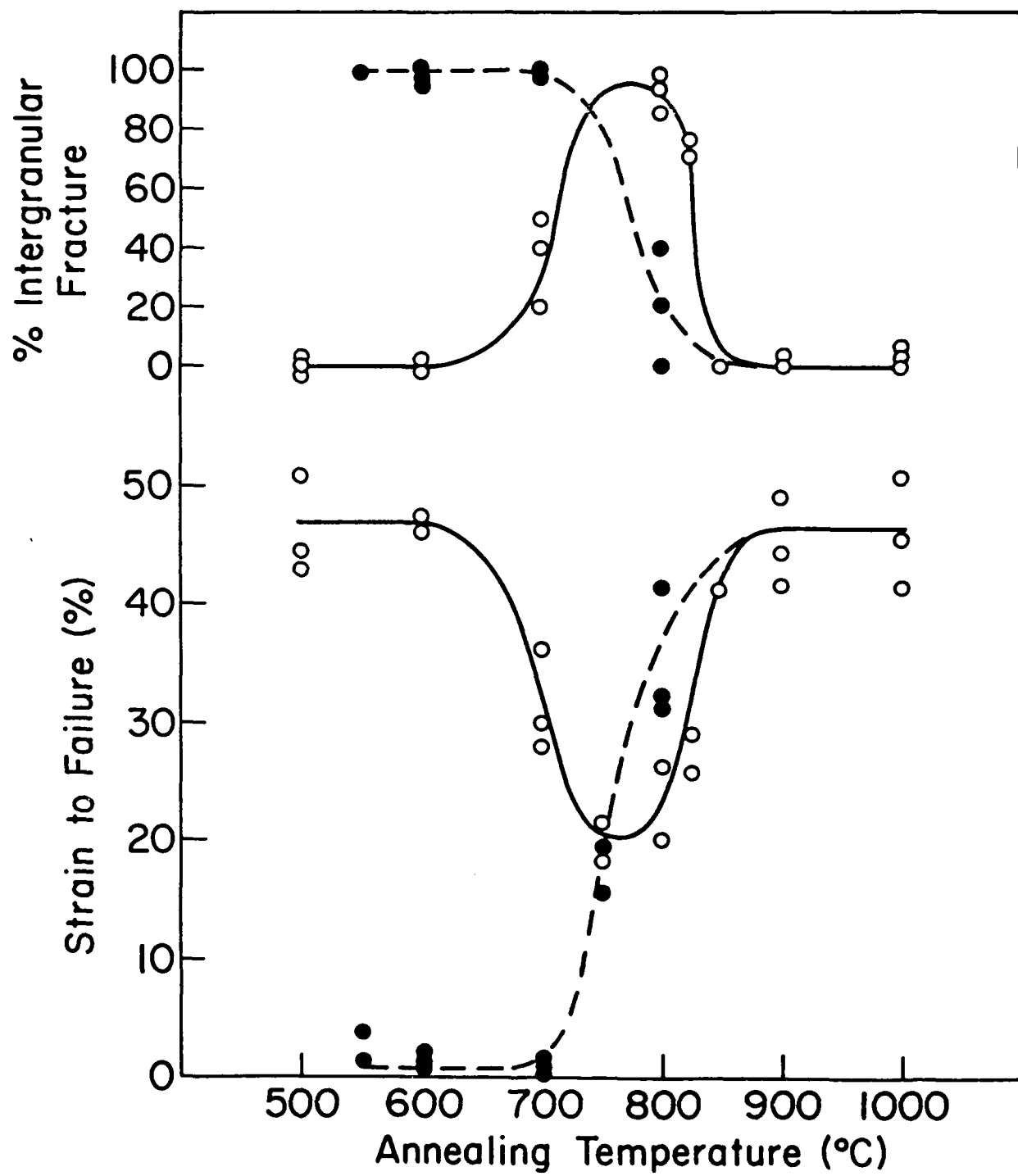


Fig. 4
Chu + Birnbaum

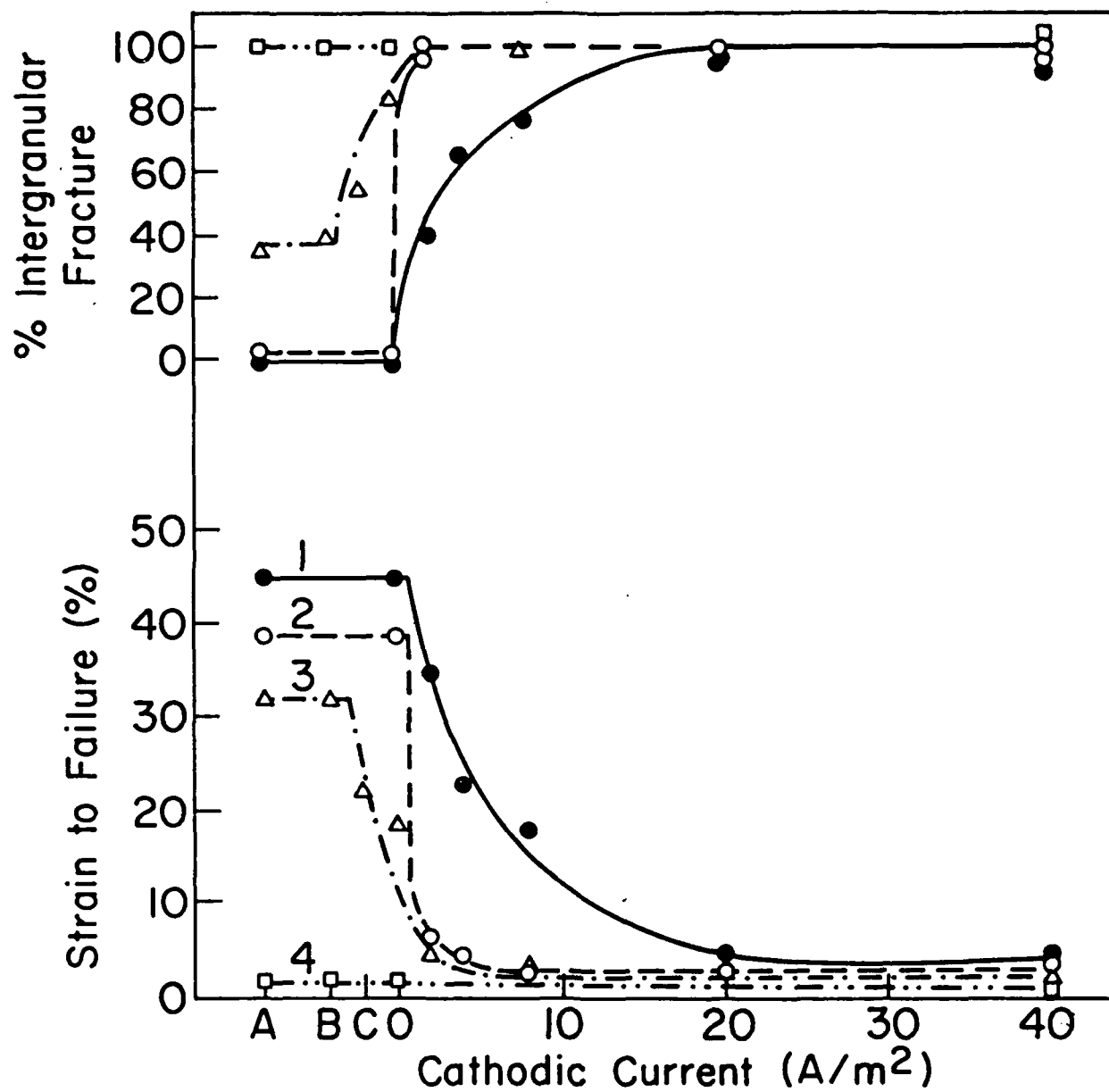


Fig. 5
Chu + Birnbaum

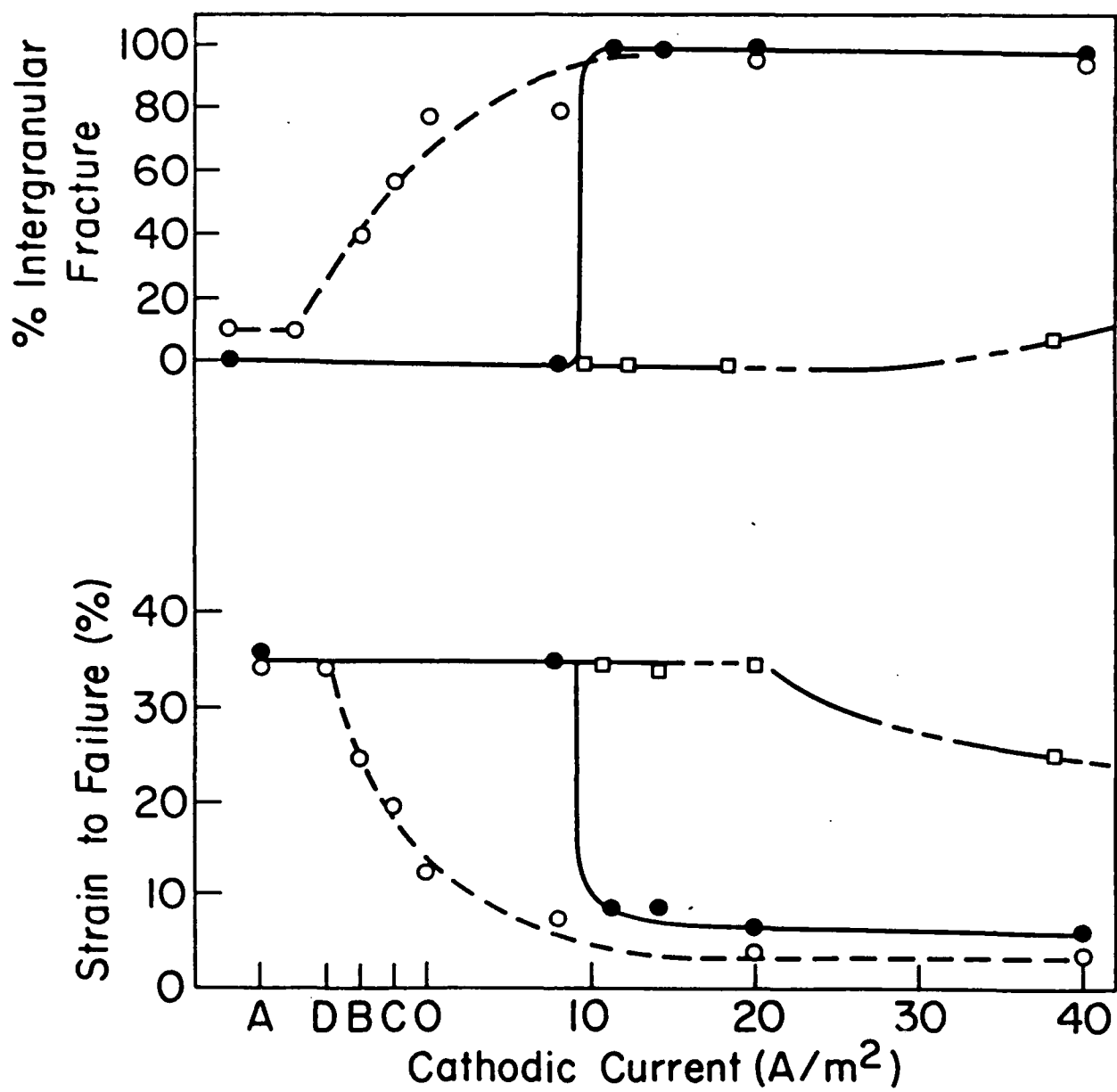


Fig. 6
Chu & Birnbaum

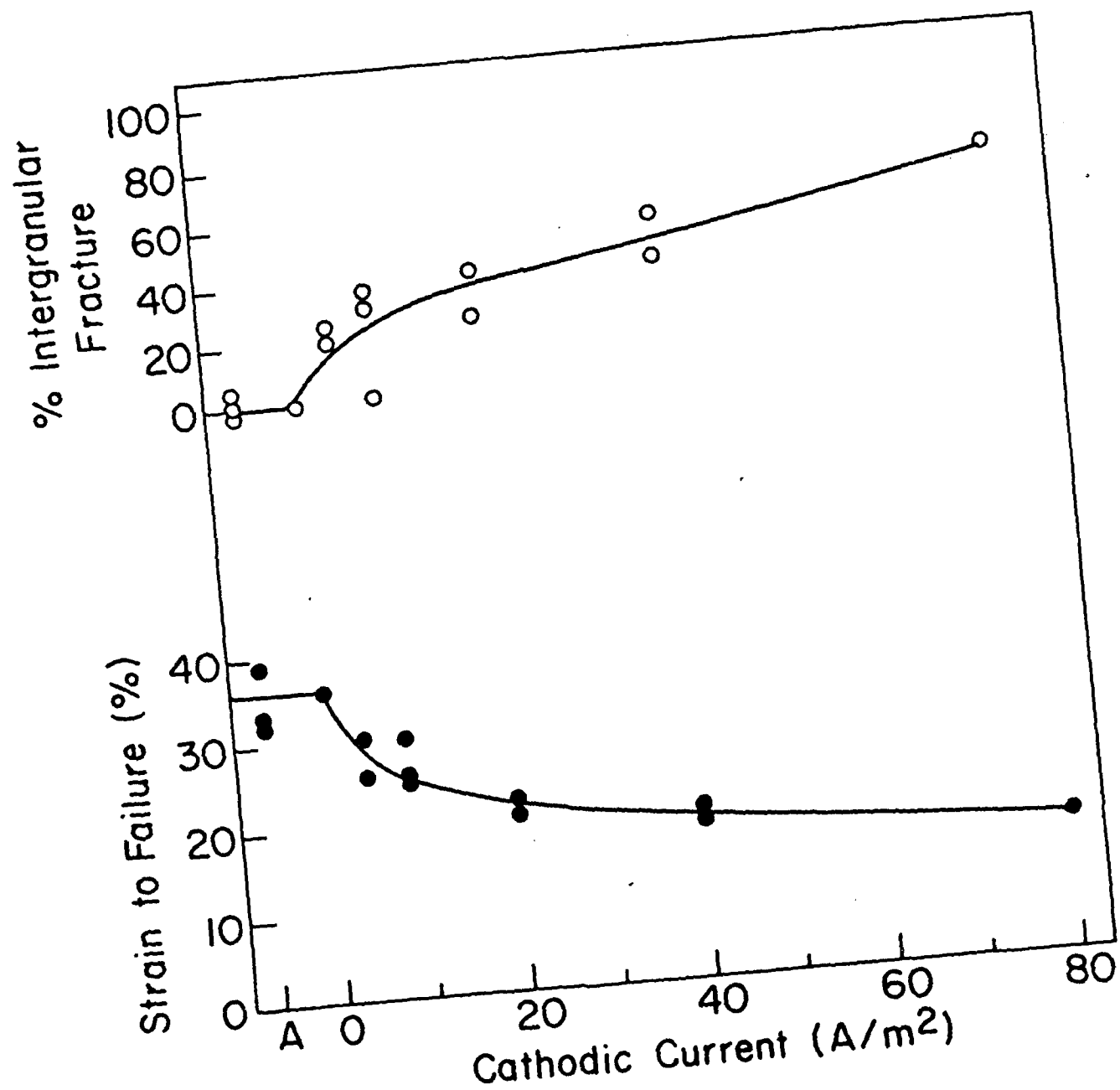


Fig. 7
Chu & Birnbaum

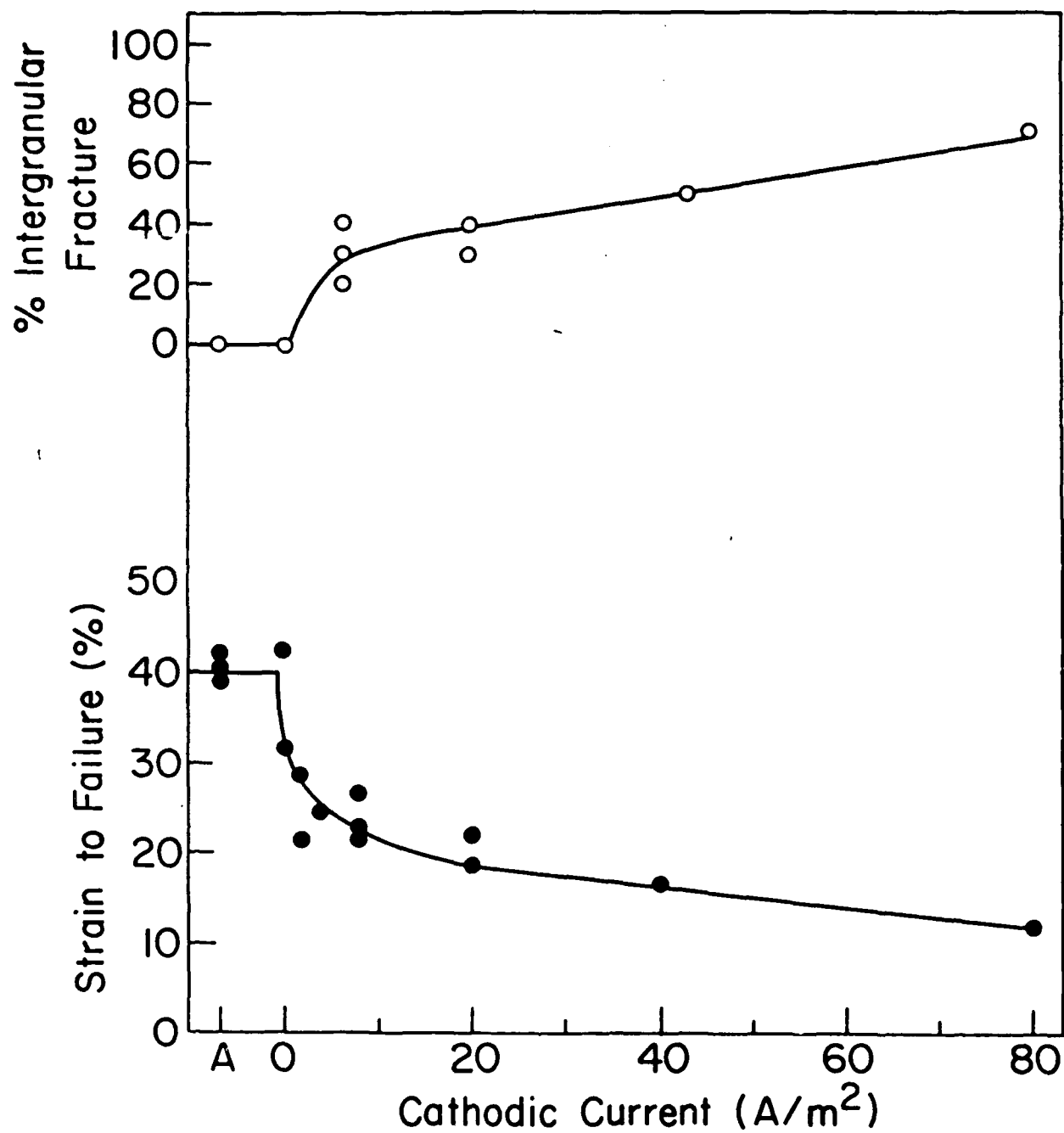


Fig. 8
Chu & Birnbaum

REPORT DOCUMENTATION PAGE		READ INSTRUCTIONS BEFORE COMPLETING FORM
1. REPORT NUMBER	2. GOVT ACCESSION NO.	3. RECIPIENT'S CATALOG NUMBER
4. TITLE (and Subtitle) Hydrogen Embrittlement of Iron-Nickel Alloys		5. TYPE OF REPORT & PERIOD COVERED Technical Report
		6. PERFORMING ORG. REPORT NUMBER
7. AUTHOR(s) W.Y. Chu and H.K. Birnbaum		8. CONTRACT OR GRANT NUMBER(s) USN 00014-83-K-0468
9. PERFORMING ORGANIZATION NAME AND ADDRESS University of Illinois, Depat. of Materials Science and Engineering, Urbana, IL 61801		10. PROGRAM ELEMENT, PROJECT, TASK AREA & WORK UNIT NUMBERS
11. CONTROLLING OFFICE NAME AND ADDRESS Office of Naval Research Arlington, VA		12. REPORT DATE April 1988
		13. NUMBER OF PAGES
14. MONITORING AGENCY NAME & ADDRESS (if different from Controlling Office)		15. SECURITY CLASS. (of this report) Unclassified
		15a. DECLASSIFICATION/DOWNGRADING SCHEDULE
16. DISTRIBUTION STATEMENT (of this Report) This document is unclassified. Reproduction and distribution for any purpose of the US Government is permitted.		
17. DISTRIBUTION STATEMENT (of the abstract entered in Block 20, if different from Report)		
18. SUPPLEMENTARY NOTES		
19. KEY WORDS (Continue on reverse side if necessary and identify by block number) Hydrogen embrittlement Iron-nickel alloys Fracture Deformation		
20. ABSTRACT (Continue on reverse side if necessary and identify by block number) The effects of hydrogen on the deformation and fracture of alloys in the Fe-Ni alloy system were studied as a function of the alloy composition and the amount of sulfur segregated to the grain boundaries. A ductile to brittle transition in the tensile parameters and in the fracture mode was observed as the hydrogen fugacity was increased during the deformation. The variation of this transition fugacity with segregated sulfur and with alloy		

Unclassified

SECURITY CLASSIFICATION OF THIS PAGE (When Data Entered)

concentration was studied. The results were related to the mechanisms proposed for hydrogen related fracture of metals.

Unclassified

SECURITY CLASSIFICATION OF THIS PAGE(When Data Entered)

END

DATE

FILMED

9-88

DTIC